

OPTIMIZATION-BASED MOTION PRIMITIVE AUTOMATA FOR AUTONOMOUS DRIVING

MATHEUS V. A. PEDROSA ¹, PATRICK SCHEFFE ², BASSAM ALRIFAEI ² AND
KATHRIN FLASSKAMP ¹

¹ *Chair of Systems Modeling and Simulation, Systems Engineering, Saarland University, Germany*

² *Chair for Embedded Software, RWTH Aachen University, Germany*

ABSTRACT. Trajectory planning for autonomous cars can be addressed by primitive-based methods, which encode nonlinear dynamical system behavior into automata. In this paper, we focus on optimal trajectory planning. Since, typically, multiple criteria have to be taken into account, multiobjective optimization problems have to be solved. For the resulting Pareto-optimal motion primitives, we introduce a universal automaton, which can be reduced or reconfigured according to prioritized criteria during planning. We evaluate a corresponding multi-vehicle planning scenario with both simulations and laboratory experiments.

1. INTRODUCTION

Optimization-based control techniques play a crucial role in autonomous driving. Focusing on trajectory generation, we apply a graph-based planning method based on motion primitives, where optimization criteria can be considered at all stages of the method, i.e., the construction of the primitives and the motion planning. For computing motion primitives, we formulate multiobjective optimal control problems. The special structure-preserving primitives, named *trims*, are equipped with unit costs, which can be evaluated for selecting a set of representative trims. While classical, continuous-time optimal control does not easily allow for switching objectives, the graph-based approach introduces dynamic waypoints via the trim primitives, at which prioritization of criteria, defined by the cost and heuristic functions, can be switched [1]. However, the multi-objective design choices lead to different automata (graphs), and including Pareto-optimal motion primitives strongly influences the size of each automaton. Thus, we evaluate and compare the performance of different subgraphs of a general-purpose automata, named *universal automata*, in simulation and

E-mail address: {matheus.pedrosa, kathrin.flasskamp}@uni-saarland.de, {scheffe, alrifaee}@embedded.rwth-aachen.de.

This research is supported by the Deutsche Forschungsgemeinschaft (German Research Foundation) within the Priority Program SPP 1835 “Cooperative Interacting Automobiles” (grant number: KO 1430/17-1).

experiments in the Cyber-Physical Mobility Lab (CPM Lab), an open-source platform for networked and autonomous vehicles [2].

2. PRELIMINARIES

Motion planning with symmetry-exploiting primitives has been proposed by Frazzoli et al. in [3] as a general concept. For shortness, we summarize its application to vehicle planning in the following.

We consider the kinematic single-track (KST) model for the vehicles with the state vector $x = [s_x \ s_y \ \psi \ v \ \delta]^T \in \mathcal{M} \subset \mathbb{R}^5$, and the input vector: $u = [u_{\dot{v}} \ u_{\dot{\delta}}]^T \in \mathbb{R}^2$, where s_x and s_y are the positions of the center of gravity (CG), ψ is the vehicle orientation, v is the velocity, δ is the steering angle, \mathcal{M} is the 5-dim state manifold, $u_{\dot{v}}$ is the longitudinal acceleration, and $u_{\dot{\delta}}$ is the velocity of the steering angle. The dynamics are given by:

$$\dot{x}(t) = f(x(t), u(t)) := \begin{bmatrix} v(t) \cdot \cos(\psi(t) + \beta(t)) \\ v(t) \cdot \sin(\psi(t) + \beta(t)) \\ \frac{v(t)}{L} \cdot \tan(\delta(t)) \cos(\beta(t)) \\ u_{\dot{v}}(t) \\ u_{\dot{\delta}}(t) \end{bmatrix} \quad (1)$$

with $\beta(t) = \tan^{-1}(\frac{l_r}{L} \tan(\delta(t)))$, where L is the wheelbase length and l_r is the length from the rear axle to the CG [4].

For any given control signal u on $[0, T]$, motions are invariant w.r.t. combined translations and rotations, i.e., let $x(t) = \varphi_u(x_0, t)$ denote the trajectory starting at time $t = 0$ in x_0 , then it holds $\varphi_u(\Psi_g(x_0), t) = \Psi_g(\varphi_u(x_0, t))$ for all $t \in [0, T]$ with $g = (\Delta s_x \ \Delta s_y \ \Delta \psi)$ and

$$\Psi_g(x) = \begin{bmatrix} \cos(\Delta \psi) & -\sin(\Delta \psi) & 0 \\ \sin(\Delta \psi) & \cos(\Delta \psi) & 0 \\ 0 & 0 & 1 \end{bmatrix} \begin{bmatrix} s_x \\ s_y \\ \psi \end{bmatrix} + \begin{bmatrix} \Delta s_x \\ \Delta s_y \\ \Delta \psi \end{bmatrix}; \quad [v \ \delta]^T,$$

see e.g. [5, 6] for a proof. The equality above describe the symmetry property. In turn, all trajectories being equal up to the shift by Ψ_g for all $g \in \mathcal{G}$, i.e. the symmetry group, are summarized in the equivalence class called *motion primitive*.

A special class of motion primitives are those with fixed – i.e. trimmed – control, called *trim primitives*, which possess an analytic expression thanks to symmetry, cf. [3]. For the KST model, any motion with constant longitudinal velocity and fixed steering angle, i.e. $u_{\dot{v}}(t) = u_{\dot{\delta}}(t) = 0$ satisfies this condition. Omitting technical details, these motions belong to either ”driving straight with constant velocities” or ”driving on arcs of circles with constant velocities”.

Motion primitives can be *concatenated*, if symmetry shifts Ψ_g can be used to map a successor’s starting point to the predecessors ending point (again, cf. [3] or the authors’ previous works for details). For switching between one trim primitive to another, a special connecting primitive is needed; e.g., it can accelerate, decelerate or adjust the steering angle. This kind of primitive is named *maneuver*. Thus, maneuvers typically require highly controlled motion,

so that optimal control is a suitable tool to compute maneuvers (see Sect. 3). Sequences of motion primitives which form valid trajectories of Eq. (1) alternate between trim primitives and maneuvers.

Finally, the idea of motion planning with primitives is to restrict to a *finite set of motion primitives* and solve a given planning problem by finding the best sequence within this set. Given the distinction into trim primitives and maneuvers, it is convenient to represent the finite set of motion primitives by a graph [3]. The trims are represented by the vertices of the graph, while the maneuvers, by the edges. For a fully state/control-quantized and time-discretized setting, also the duration of trims is defined to be fixed.

3. OPTIMAL MOTION PRIMITIVE AUTOMATON DESIGN

Selection strategies for trims to be considered in the motion primitive graph that can be found in the literature are, e.g., an arbitrary choice according to the expected operating points [7, 8] or detecting the most representative trims from a dataset [6]. Complementarily, we focus on the optimization criteria here. Let $J(T, x, u) = \int_0^T \ell(x(t), u(t)) dt$ be a cost function with running cost $\ell(\cdot, \cdot)$, i.e. any criterion depending on a state-control pair, which is also invariant w.r.t. Ψ_g , the system dynamics' symmetry. Then, for state-control signals (\tilde{x}, \tilde{u}) being trim primitives, it holds that

$$J(T, \tilde{x}, \tilde{u}) = T \cdot \ell(\tilde{x}(0), \tilde{u}(0)) = T \cdot \ell(\tilde{x}(0), 0).$$

While the first equality is due to trim definition ($\tilde{u}(t) = \text{const.}$, in particular) and invariance (see [7, Prop. 4]), the second simplification holds for the KST model, since any trim satisfies $\tilde{u} \equiv 0$. $\ell(\tilde{x}(0), \tilde{u}(0))$ is called *unit cost* in [3].

To obtain maneuvers that are optimal with respect to multiple criteria J_1, \dots, J_K , $K > 1$, the following multiobjective optimal control problem (MOCP) can be solved:

$$\underset{T, x, u}{\text{minimize}} \quad [J_1(T, x, u) \quad \dots \quad J_K(T, x, u)]^\top \quad (2a)$$

$$\text{subject to} \quad \dot{x}(t) = f(x(t), u(t)), \quad 0 < t \leq T, \quad \text{cf. Eq. (1),} \quad (2b)$$

$$0 = r(x(0), x(T)), \quad (2c)$$

$$0 \geq g(x(t), u(t)), \quad 0 < t \leq T, \quad (2d)$$

with boundary constraints $r(x(0), x(T))$ assuring the connection of trims, and $g(\cdot)$ for any type of state/input constraints in between.

In autonomous driving, different kinds of objectives may play a role, e.g.:

- Travel time: not only in transportation of goods, minimizing travel time corresponds to higher profits.
- Effort: saving energy is of critical importance when the fuel or the battery is close to empty, or for reducing monetary costs.
- Safety: emergency maneuvers can be needed for critical situations [9].

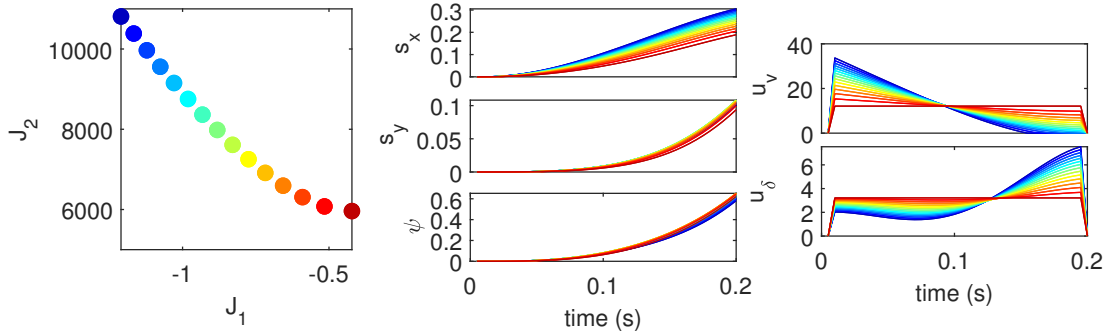


FIGURE 1. Example of a Pareto set with respective positions, orientations, and inputs for a maneuver going from a trim with zero speed and steering angle to $v = 2.3 \text{ m s}^{-1}$ and $\delta = 0.62 \text{ rad}$. It was considered the KST model with $J_1 = -\int_0^T (\|s_x\|_2^2 + \|s_y\|_2^2) dt$ and $J_2 = \int_0^T \|u\|_2^2 dt$, for a fixed duration $T = 0.2 \text{ s}$, and the parameters used in the evaluation.

- Passengers' comfort: typically modeled via acceleration minimization or by avoiding sickness-proven eigenmodes in multi-body systems for car-human models. It is assumed that autonomous driving should improve safety without losing too much comfort or utility [9].

In Fig. 1, we show an example of a Pareto set for maneuvers going from a trim with $v = 0 \text{ m s}^{-1}$ and $\delta = 0 \text{ rad}$ to $v = 2.3 \text{ m s}^{-1}$ and $\delta = 0.62 \text{ rad}$, but computed with different cost functionals. It was considered the same constraints for the model-scale vehicle used in the evaluation [4]. The duration was a fixed parameter, as a requirement to be explained in the next section. The Pareto set shows a trade-off between travel time in J_1 and effort/comfort in J_2 . Note that the maneuvers in blueish colors show a longer traveled distance with high control inputs in opposition to soft inputs for a smaller distance in the reddish points.

Following the strategies for obtaining primitives mentioned above, we can define a general-purpose automaton named *universal automaton (UA)* (see Fig. 2). It can include many trim primitives, and, in particular, the Pareto-optimal maneuvers for connecting pairs of those trims [1]. Along the way, the UA can reconfigure its size and operation mode by enabling/disabling some trims and/or maneuvers. Firstly, it can restrict the trims to respect, for example, the allowed speed at a certain road. Second, choosing the objective J_k ($1 \leq k \leq K$), which is currently of prior importance at the time of the planning task. Then, planning is performed on the subgraph only consisting of the maneuvers optimal to J_k .

For the planning algorithm via graph search, the cost and heuristic functions could follow the reconfiguration of the UA and be aligned to the choice of J_k . In this work, these functions will be kept constant as given in [5], since our focus is on the automaton design, rather than on the parameters of the planning method.

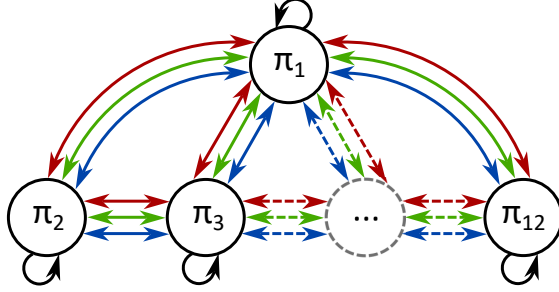


FIGURE 2. The universal automaton used in the evaluation for the trims given in Tab. 1. Blue maneuvers were computed for J_1 , red ones were computed for J_2 , and green ones, for J_3 . Bidirectional arrows represent two maneuvers, one in each direction.

4. EVALUATION AND RESULTS

We evaluate the different automata in simulations and experimentally. In a simulator of the CPM Lab, we test three vehicles driving in collision route as illustrated in Fig. 3. The car depicted in red drives a figure-eight path, while the ones depicted in blue and green drive a circular path on the lower half and the right half of the map, respectively. In the CPM Lab, we evaluate the trajectory just for the car depicted in red. The simulations run on a laptop with 1.9 GHz Intel[®] Core[™] i7 CPU and 16 GB RAM.

The CPM Lab is a 1:18-scale, open-source platform for up to 20 networked and autonomous vehicles, the μ Cars, for applications and tests on networked decision-making, trajectory planning, and control [2]. It runs trajectory planning algorithms on an AMD Ryzen[™] 5 5600X 6-core 3.7 GHz CPU and 32 GB of RAM machine. It replicates a wide variety of common traffic scenarios with a 16-lane urban intersection, a highway, highway on-ramps, and highway off-ramps.

The used planning algorithm is an extension of the receding horizon graph search (RHGS) algorithm, presented in [5], using prioritized distributed model predictive control (DMPC) [10, 11]. The RHGS merges the motion primitive graph search with a receding horizon framework while ensuring recursive feasibility. We consider a prediction horizon of 8 time steps and a time step duration of 0.2 s. Therefore, all maneuvers are computed for a fixed duration of 0.2 s.

The UA design is shown in Fig. 2 with trims given in Tab. 1 and maneuvers computed optimization-based w.r.t. $J_1 = -\int_0^T (\|s_x\|_2^2 + \|s_y\|_2^2) dt$, $J_2 = \int_0^T \|u\|_2^2 dt$ and $J_3 = 0.5J_1 + 0.5J_2$ (see Fig. 1 for a compromise between these costs), using the KST model, initial states with zero values and respecting the constraints imposed by the μ Cars [12]. We evaluate the UA in four configurations: subgraph A (B, C, respectively) has all trims and optimal maneuvers w.r.t. J_1 (J_2 , J_3 , resp.); subgraph D contains trims π_i , $i = 1, 2, 4, 6, 7, 8, 10, 12$, and optimal maneuvers w.r.t. J_3 . When positioned side by side, the subgraphs A, B, and C compare different Pareto-optimal maneuvers, while C and D compare subgraphs of different sizes.

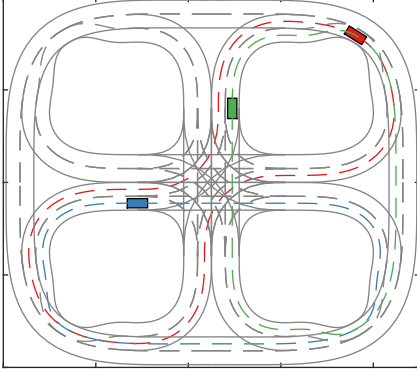


FIGURE 3. Test scenario for three cars.

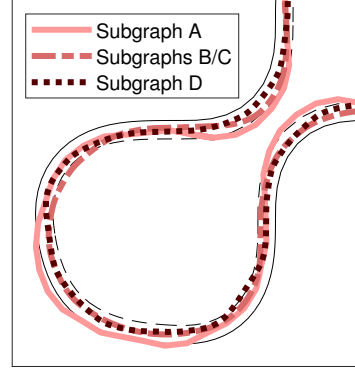


FIGURE 4. Simulation of the red vehicle.

TABLE 1. Trim primitives of the universal automaton.

Trim ID	π_1	π_2	π_3	π_4	π_5	π_6	π_7	π_8	π_9	π_{10}	π_{11}	π_{12}
v [m s ⁻¹]	0	0.4	0.5	0.6	0.7	0.8	0.8	0.8	0.7	0.6	0.5	0.4
δ [rad]	0	-0.60	-0.48	-0.36	-0.24	-0.12	0	0.12	0.24	0.36	0.48	0.60

Tab. 2 shows the numerical results for 150 steps, totaling 30 s. We evaluate the performance through the deviation from the aimed center of the lane. Also, the time to complete one lap is of interest. These two evaluation parameters are from the red vehicle of Fig. 3. The trajectories for this vehicle in the simulation can be seen in Fig. 4, in which the results for the subgraphs B and C are essentially similar. The necessary computational burden is given by the number of expanded vertices during the search. Finally, the max. computation time indicates the complexity of the respective subgraph.

Subgraph A shows the poorest performance. Since these maneuvers have the largest displacements, they can hardly track the center lane. Due to this fact, planning in real-time failed for subgraph A. Subgraphs B and C give different results in the CPM Lab, which indicates that a single change in the selected Pareto-optimal maneuvers of the UA influences the graph search results. Subgraph D presents a reduced number of expanded vertices when compared to C, which reduces its computation times. At the cost of a slightly larger max. computation time, a solution with less deviation to the center lane is found in subgraph D, despite providing fewer trims and maneuvers here.

5. CONCLUSIONS

In this paper, we describe the construction of a motion primitive automaton with Pareto-optimal motion primitives. We evaluate four configurations of a generic automaton in both simulation and experiments in the CPM Lab, for multiple vehicles, in a prioritized DMPC scheme. The results show that the choice of primitives and their optimization criteria play a role in the planning's real-time capability, trajectory performance, computation time, and

TABLE 2. Results, where mean values are followed by standard deviations in parentheses.

Subgraph	A		B		C		D	
	Simulation	CPM Lab	Simulation	CPM Lab	Simulation	CPM Lab	Simulation	CPM Lab
Reference error* [mm]	40.1 (35.9)	27.9 (30.5)	30.7 (28.9)	27.9 (30.5)	30.8 (28.8)	19.9 (23.7)	19.4 (17.6)	17.0 (16.1)
Time for one lap [s]	13.8	15.8	15.8	15.8	15.8	16.0	16.2	16.0
Max. expanded vertices	159114	430	1966	430	1969	322	879	291
Computation time [ms]	9738.3 (5228.1)	12.4 (3.8)	125.0 (67.5)	12.4 (3.8)	166.5 (80.1)	11.8 (3.1)	138.4 (71.2)	10.2 (3.3)
Max. comp. time [ms]	28436.7	32.3	600.9	32.3	570.7	24.5	654.4	32.8

* Euclidean distances to the center of the lane.

speed of the vehicles, causing the need for a trade-off between these criteria. Future work can evaluate a reconfiguration of the automaton in real-time, based on a dynamic objective's prioritization.

REFERENCES

- [1] K. Flaßkamp, *On the Optimal Control of Mechanical Systems – Hybrid Control Strategies and Hybrid Dynamics*. PhD thesis, University of Paderborn, 2013.
- [2] M. Kloock, P. Scheffe, J. Maczijekowski, A. Kampmann, A. Mokhtarian, S. Kowalewski, and B. Alrifaae, “Cyber-Physical Mobility Lab: An open-source platform for networked and autonomous vehicles,” in *2021 European Control Conference (ECC)*, pp. 1937–1944, 2021.
- [3] E. Frazzoli, M. A. Dahleh, and E. Feron, “Maneuver-based motion planning for nonlinear systems with symmetries,” *IEEE Transactions on Robotics*, vol. 21, no. 6, pp. 1077–1091, 2005.
- [4] M. Althoff, M. Koschi, and S. Manziinger, “Commonroad: Composable benchmarks for motion planning on roads,” in *Proc. of the IEEE Intelligent Vehicles Symposium*, 2017.
- [5] P. Scheffe, M. V. A. Pedrosa, K. Flaßkamp, and B. Alrifaae, “Receding horizon control using graph search for multi-agent trajectory planning,” *IEEE Transactions on Control Systems Technology*, pp. 1–14, 2022.
- [6] M. V. A. Pedrosa, T. Schneider, and K. Flaßkamp, “Learning motion primitives automata for autonomous driving applications,” *Mathematical and Computational Applications*, vol. 27, no. 4, 2022.
- [7] K. Flaßkamp, S. Ober-Blöbaum, and K. Worthmann, “Symmetry and motion primitives in model predictive control,” *Math. Control. Signals Syst.*, vol. 31, pp. 455–485, 2019.
- [8] M. V. A. Pedrosa, T. Schneider, and K. Flaßkamp, “Graph-based motion planning with primitives in a continuous state space search,” in *2021 6th International Conference on Mechanical Engineering and Robotics Research (ICMERR)*, pp. 30–39, 2021.
- [9] M. Naumann, M. Lauer, and C. Stiller, “Generating comfortable, safe and comprehensible trajectories for automated vehicles in mixed traffic,” in *2018 21st International Conference on Intelligent Transportation Systems (ITSC)*, pp. 575–582, 2018.
- [10] P. Scheffe, G. Dorndorf, and B. Alrifaae, “Increasing feasibility with dynamic priority assignment in distributed trajectory planning for road vehicles,” in *2022 IEEE 25th International Conference on Intelligent Transportation Systems (ITSC)*, pp. 3873–3879, 2022.
- [11] B. Alrifaae, F.-J. Heßeler, and D. Abel, “Coordinated non-cooperative distributed model predictive control for decoupled systems using graphs,” *IFAC-PapersOnLine*, vol. 49, no. 22, pp. 216–221, 2016.
- [12] P. Scheffe, J. Maczijekowski, M. Kloock, A. Kampmann, A. Derks, S. Kowalewski, and B. Alrifaae, “Networked and autonomous model-scale vehicles for experiments in research and education,” *IFAC-PapersOnLine*, vol. 53, no. 2, pp. 17332–17337, 2020.